Methionine-induced hyperhomocysteinemia impairs the antioxidant ability of high-density lipoproteins without reducing in vivo macrophage-specific reverse cholesterol transport

ARTICLE *in* MOLECULAR NUTRITION & FOOD RESEARCH · JUNE 2013

Impact Factor: 4.6 · DOI: 10.1002/mnfr.201300133

RESEARCH ARTICLE

Methionine-induced hyperhomocysteinemia impairs the antioxidant ability of high-density lipoproteins without reducing in vivo macrophage-specific reverse cholesterol transport

Josep Julve[1,2], Joan C. Escolà-Gil[1,2*], Elisabeth Rodríguez-Millán[1*], Jesús M. Martín-Campos[1,2], Matti Jauhiainen[3], Helena Quesada[1,2], Ivy M. Rentería-Obregón[1], Jesús Osada[4,5], José L. Sánchez-Quesada[1] and Francisco Blanco-Vaca[1,2,6]*

[1] Institut d'Investigacions Biomèdiques Sant Pau (IIB-Sant Pau), Barcelona, Spain
[2] CIBER de Diabetes y Enfermedades Metabólicas Asociadas, CIBERDEM, Spain
[3] National Institute for Health and Welfare, Public Health Genomics Unit, Biomedicum, Helsinki, Finland
[4] CIBER de Fisiopatología de la Obesidad y Nutrición, Instituto de Salud Carlos III, Madrid, Spain
[5] Departamento de Bioquímica y Biología Molecular y Celular, Facultad de Veterinaria, Instituto de Investigación Sanitaria de Aragón, Universidad de Zaragoza, Zaragoza, Spain
[6] Departament de Bioquímica i Biologia Molecular, Universitat Autònoma de Barcelona, Barcelona, Spain

Received: February 20, 2013
Revised: March 26, 2013
Accepted: March 31, 2013

Scope: High plasma homocysteine concentrations have been associated with increased risk of cardiovascular disease both in humans and experimental animal models, whereas plasma HDL-cholesterol concentration is inversely correlated with such disorders. This work aimed to study the impact of methionine-induced hyperhomocysteinemia (HHcy) on two major antiatherogenic functions of HDL, namely their capacity to prevent LDL oxidation and induce in vivo macrophage-specific reverse cholesterol transport.

Methods and results: Methionine-induced HHcy in mice resulted in an approximately 20% decreased concentration of HDL-cholesterol and HDL main protein component, apolipoprotein A-I. The HDL potential to resist oxidation as well as to prevent LDL oxidative modification was impaired in hyperhomocysteinemic mice. Activities of paraoxonase-1 and platelet activation factor acetylhydrolase, two of the main HDL-associated enzymes with antioxidant activity, were reduced. The ability of HDL to efflux cholesterol from macrophages was decreased in hyperhomocysteinemic mice; however, the in vivo macrophage-specific reverse cholesterol transport measured as the output of labeled cholesterol into feces did not significantly differ between groups.

Conclusion: Our data indicate that the HDL from methionine-induced hyperhomocysteinemic mice was more prone to oxidation and displayed lower capacity to protect LDL against oxidative modification than that of control mice, highlighting a mechanism by which a diet-induced HHcy may facilitate progression of atherosclerosis.

Keywords:
HDL / Homocysteine / Hyperhomocysteinemia / Methionine / Oxidation / Reverse cholesterol transport

Correspondence: Dr. Josep Julve, Hospital de la Santa Creu i Sant Pau, Servei de Bioquímica, C/Sant Quintí 89, 08041 Barcelona, Spain
E-mail: jjulve@santpau.cat
Fax: +34-93-5537287

Abbreviations: apo, apolipoprotein; **GGE**, gel gradient electrophoresis; **Hcy**, homocysteine; **HDL-C**, HDL-cholesterol; **HHcy**, hyperhomocysteinemia; **LCAT**, lecithin-cholesterol acyltransferase; **RCT**, reverse cholesterol transport

*These authors contributed equally to this work.

Additional corresponding author: Dr. Francisco Blanco-Vaca, E-mail: fblancova@santpau.cat

Additional supporting information may be found in the online version of this article at the publisher's web-site

1 Introduction

Dietary factors play a crucial role in atherosclerosis development and strong evidence indicates that dietary animal proteins may contribute to atherosclerosis development [1–3]. Atherogenic effects of animal proteins are related, at least in part, to a high methionine content [1, 4–6]. Methionine and an excess of animal protein intake is considered as a possible risk factor for coronary artery disease; in contrast, lowering methionine intake may increase life span [6, 7]. Consumption of methionine-rich foods can affect plasma homocysteine (Hcy) concentration as methionine is the only known source of Hcy, a nonprotein-forming sulfur amino acid intermediate in the methylation and transsulfuration pathways [8]. The increase in plasma Hcy (termed hyperhomocysteinemia [HHcy]) can be explained by nutritional or genetic disorders in its metabolism [9–11]. In humans, normal fasting plasma concentration of Hcy is usually between 7 and 14 μM. Moderate HHcy (defined as fasting plasma concentration of Hcy between 14 and 30 μM) [12] affects around 5–10% of healthy subjects [9] but 20–40% of patients with cardiovascular disease [1], and is considered a risk factor for cardiovascular diseases [9, 13, 14]. However, Hcy-lowering therapies based on folic acid and/or vitamin B fortification failed to demonstrate any benefit in patients with established vascular disease [15]. Therefore, it remains unclear whether HHcy itself could play a causative role in the onset of vascular diseases or is merely a biomarker of such diseases.

HHcy induced by methionine supplementation can accelerate atherosclerotic lesion development under proatherogenic dietary conditions [9]. Suggested mechanisms include a wide and complex array of altered processes including impairment of vascular endothelial function, promotion of vascular smooth muscle cell proliferation, enhancement of monocyte and leukocyte infiltration, stimulation of inflammatory cytokine expression, increase in lipid peroxidation, oxidative modification of lipoproteins, and induction of atherosclerosis and thrombosis (reviewed in [9, 16–18]). Since HDLs and apolipoprotein (apo)A-I are well-recognized cardioprotective elements [19], a relevant pathophysiologic question is whether HHcy influences the antiatherogenic functions of HDL [19, 20], particularly, considering that HHcy is commonly associated with decreased plasma HDL-cholesterol (HDL-C) concentration in both animal models [20–25] and humans [20, 23, 24, 26]. Some studies determined that HHcy reduced HDL-mediated cellular cholesterol efflux ability (the first step in reverse cholesterol transport [RCT]) in vitro [9, 20]. Therefore, the present study aimed to determine the effect of HHcy induced by a methionine-rich diet on two major antiatherogenic HDL functions: macrophage-specific RCT and protection against LDL oxidation.

2 Materials and methods

2.1 Mice and treatment

C57BL/6NCrl mice were obtained from Charles River Laboratories International, Inc. (strain code 027; Bar Harbour, ME, USA). At the beginning of the study, 2-month-old female mice were randomized into two groups and maintained on a regular chow diet (A04 rats and mice maintenance diet, Scientific Animal Food & Engineering, Augy, France) containing 3.1% fat and 0.02% cholesterol for 12 wk. The exact formulation of this diet is shown in Table 1. HHcy was induced by 1% v/v methionine supplementation to the drinking water, changed every 2 days, for the same period. We determined the daily food and drink intake individually (Supporting Information Table 1) and used these values to estimate the daily intake of methionine in mice (Table 1). In some experiments, 2-month-old male mice of the same strain were also randomized and maintained under the described conditions. Animals were kept in a temperature-controlled (20°C) room with a 12-h light/dark cycle. Food and water were provided ad libitum. When indicated, fasting was triggered by 6-h food deprivation prior to a blood sample being taken from each mouse. Mice were euthanized and exsanguinated by cardiac puncture. All animal procedures adhered strictly to the published recommendations of the Guide for the Care and Use of Laboratory Animals [27] and were reviewed and approved by the Institutional Animal Care and Use Committee of the Institut de Recerca de l'Hospital de la Santa Creu i Sant Pau, IIB-Sant Pau and the Department d'Agricultura, Ramaderia, Pesca, Alimentació i Medi Natural (Generalitat de Catalunya).

2.2 Biochemical analyses

The methods used for plasma and lipoprotein lipid analyses have been described in detail elsewhere [28]. Plasma Hcy concentration was determined using a commercial Hcy Assay Kit from Abbott adapted to an Architect ci16200 (Abbott Diagnostics, Irving, TX, USA). Plasma lipids, alanine transaminase (ALT), and aspartate transaminase (AST) activities were determined using commercial kits adapted to a COBAS c501 autoanalyzer (Roche Diagnostics, Germany) [28]. Mouse apoA-I was quantified by an ELISA assay, as previously reported [29]. Lipoprotein fractions,

Table 1. Diet composition and approximate daily intakes of amino acid and gross components per mouse

	A04 diet (g/kg)	CTRL (mg/day)	MET (mg/day)
Protein	161.0	853.3	821.1
Arginine	9.8	51.9	50.0
Cystine	2.3	12.2	11.7
Lysine	7.7	40.8	39.3
Methionine	2.8	14.8	64.3[a)]
Tryptophan	1.9	10.1	9.7
Glycine	8.1	42.9	41.3
Carbohydrate E.N.A.	600.0		
Fiber	40.0		
Fat	31.0		
Palmitic acid (16:0)	4.0		
Palmitoleic acid (16:1)	0.6		
Oleic acid (18:1)	6.4		
Linoleic acid (18:2)	12.4		
Linolenic acid (18:3)	0.09		
Vitamin A (IU/kg)	6600.0		
Vitamin D3 (IU/kg)	900.0		
Vitamin E	0.03		
Folate	0.0005	2.7	2.6

a) Note the increase in methionine (i.e. solid methionine intake 14.3 mg/day + liquid methionine intake 50.0 mg/day = total methionine intake 64.3 mg/day) shown in the hyperhomocysteinemic mice.
A04 rats and mice maintenance diet, Scientific Animal Food & Engineering; values expressed as gram per kilogram of diet, except for vitamins A and D3 that are expressed as IU/kg diet; approximate values of daily intake per mouse expressed as milligram per day, except for folate content that is expressed as microgram per day. For comparison of gross diet component intake and amino acid content, including methionine, between groups, values were calculated based on their daily food and water intake, respectively (see online Table 1). CTRL, control mice; MET, methionine-induced hyperhomocysteinemic mice.

including HDL, were separated by a Fast Protein Liquid Chromatography system using a Superose 6® column (GE Healthcare, Buckinghamshire, UK) [28] and cholesterol was measured in each eluted fraction. HDL was also isolated by sequential ultracentrifugation at 100 000 × *g* for 24 h [28]. HDL composition, including total and free cholesterol, triglycerides, and phospholipids, was determined by commercial methods adapted to a COBAS c501 autoanalyzer (Roche Diagnostics). HDL protein concentrations were determined by the bicinchoninic acid method (TermoScientific, Rockford, IL, USA). HDL size was determined by nondenaturing 4–30% polyacrylamide gel gradient electrophoresis (GGE) stained with Coomassie G-250 [29]. Immunoblot analysis for mouse apoA-I in HDL was performed by separating plasma HDL by nondenaturing 4–20% polyacrylamide GGE. Proteins were blotted onto nitrocellulose membrane and incubated with mouse apoA-I-specific antibodies as described previously [30]. The amount of preβ-HDL formed during 6 h of preincubation of serum in the presence of a lecithin-cholesterol acyltransferase (LCAT) inhibitor was quantified by resolving the samples by 2D crossed immunoelectrophoresis, as previously reported [31].

2.3 Fecal and liver cholesterol analyses

Stools from individually housed mice, fed ad libitum and with free access to water were collected over 2 days. Mice were euthanized and exsanguinated by cardiac puncture at the end of the study and livers removed after being perfused extensively with saline. Lipids were extracted from 1 g of feces and 100 mg of liver, respectively, with isopropyl alcohol-hexane (2:3; v/v). After the addition of Na_2SO_4, the hexane phase was isolated, dried with nitrogen, reconstituted with 0.5% sodium cholate, and sonicated for 10 min (50 Hz) prior to lipid measurements. Liver and stools were extracted into ethanol-containing tubes for determination of total bile acid content by the 3α-hydroxysteroid dehydrogenase method (Sigma Diagnostics, St. Louis, MO, USA). Net intestinal cholesterol absorption was measured in an independent group of mice at the end of the study by a fecal dual-isotope ratio method, as previously described [29].

2.4 HDL turnover analysis

Autologous [^{3}H]-cholesteryl oleate-labeled HDL (containing 5×10^5 cpm) obtained from hyperhomocysteinemic and control mice were isolated and intravenously injected into each mouse [29]. Serum was collected into tubes at 1, 2, 6, and 24 h under isofluorane anesthesia. Serum decay curves for the tracer were normalized to radioactivity at the initial 2-min time-point after tracer injection. Fractional catabolic rates (FCR) were calculated from the area under the serum disappearance curves fitted to a nonlinear, two-phase exponential decay model [29]. The HDL-C FCR values were used to calculate the HDL-C secretion rate using the formula [(pool size × FCR)/g]. Serum volume was estimated to be 4% of body weight. At the end of the experiment, livers and feces were collected and subjected to lipid extraction. Liver and fecal [^{3}H]-tracer expressed as percentage of injected dose was also determined.

2.5 [^{3}H]-cholesterol efflux from cultured mouse macrophage foam cells

Cholesterol efflux promoted by mouse plasma and HDL was evaluated from [^{3}H]-cholesterol-labeled J774 macrophages prepared for the macrophage-specific RCT assay. Briefly, cellular cholesterol was labeled for 48 h of incubation with 2 μCi/well [1α, 2α(n)-^{3}H]-cholesterol (GE Healthcare Europe, Germany). [^{3}H]-cholesterol-labeled cells were incubated in DMEM containing 5% mouse plasma or HDL from apoB-containing lipoprotein-depleted plasma, respectively, at 37°C for 4 h. The media and cell lysates were collected and analyzed for [^{3}H]-radioactivity by liquid scintillation. Cholesterol efflux (%) was calculated as $cpm_{medium}/(cpm_{cells} + cpm_{medium}) \times 100$.

2.6 In vivo macrophage-specific RCT

Murine macrophage cell line J774 (American Type Culture Collection, Manassas, VA, USA) was cultured in 75-cm tissue culture plates at 5 million cells per plate and grown to 90% confluence in RPMI 1640 supplemented with 10% fetal bovine serum. Mouse macrophages were incubated for 48 h in the presence of 5 μCi/mL of [1α, 2α(n)-^{3}H]-cholesterol (GE Healthcare Europe GmbH), 100 μg/mL of acetylated LDL, and 10% lipoprotein-depleted serum [29]. These cells were washed, equilibrated, resuspended in 0.9% w/v saline, and pooled before being intraperitoneally injected into mice [29]. Mice were injected intraperitoneally with [^{3}H]-cholesterol-labeled J774 mouse macrophages ($\sim 3 \times 10^6$ cells containing $\sim 10^6$ cpm in 0.5 mL of saline in each mouse; cell viability was >90%, measured by Trypan Blue staining) as described [29]. Mice were individually housed in metabolic cages, and stools were collected over the next 2 days to determine the output of radioactivity associated with cholesterol per animal. At that time-point, mice were euthanized and exsanguinated by cardiac puncture and livers removed. [^{3}H]-cholesterol in plasma and HDL were determined at 48 h by liquid scintillation counting [29]. HDL-associated [^{3}H]-cholesterol was obtained after precipitation of apoB-containing lipoproteins with phosphotungstic acid and magnesium chloride (Roche Diagnostics GmbH, Germany) [28]. Liver and fecal lipids were extracted with isopropyl alcohol-hexane. The lipid layer was collected, evaporated, and [^{3}H]-tracer measured by liquid scintillation counting [29]. [^{3}H]-tracer detected in fecal bile acids was determined in the remaining aqueous portion of fecal material extracts. A known amount of [1α, 2α(n)-^{3}H]-cholesterol (GE Healthcare) and [^{3}H(G)]-taurocholic acid (PerkinElmer, CA, USA) was used as an internal control. The amount of [^{3}H]-tracer was expressed as a fraction of the injected dose.

2.7 Susceptibility to lipoprotein oxidation

Phosphate-saline buffer was changed to isolated lipoproteins by gel filtration on PD-10 columns (GE Healthcare). Oxidation was started by adding 2.5 μmol/L $CuSO_4$ to human LDL (0.1 mmol/L phospholipids) and HDL (0.1 mmol/L of phospholipids) mixtures or to LDL and HDL alone [32]. Conjugated diene formation was measured by continuous monitoring of absorbance at 234 nm in a Synergy HT microplate reader (BioTek Synergy, Winooski, VT, USA) at 37°C for 6 h. The lag phase was calculated as described [32]. Kinetics of the LDL oxidation in the LDL + HDL incubations were calculated by subtracting the kinetics of HDL incubated without LDL. In parallel, the relative electrophoretic mobility of oxidized lipoproteins was also determined. Mouse HDL (0.1 mmol/L phospholipids) were mixed with human LDL (0.1 mmol/L phospholipids) as described [32]. Briefly, oxidation was started with 2.5 μmol/L $CuSO_4$ at 37°C in the dark for 150 min. Reaction was stopped by adding 50 μmol/L EDTA and 20 μmol/L butylated hydroxytoluene and, immediately, 15 μL of lipoproteins were mixed with 5 μL of sucrose 50% and 5 μL of Sudan Black (10 g/L). This mixture (using a volume of 10 μL) were loaded onto a 0.5% agarose gel and electrophoresed at 90 V for 90 min in a cold room. Relative lipoprotein mobility was evaluated with a Chemi Doc 2000 Densitometer using the Quantity One software (Bio-Rad Laboratories SA, Life Science Group, Madrid, Spain). Results were expressed as relative LDL mobility, with the mobility of oxLDL considered as 100% and that of native LDL as 0% [32].

2.8 HDL-associated enzyme activities

Total serum arylesterase activity was measured using phenylacetate as substrate [32]. EDTA-sensitive serum arylesterase activity was calculated by subtracting the EDTA-resistant arylesterase and expressed as paraoxonase (PON)-1 activity [32]. Platelet activated factor acetylhydrolase (PAF-AH) activity was determined using a commercial kit (Cayman Chemical, Ann Arbor, MI, USA) [32]. LCAT activity toward endogenous lipoproteins labeled with radioactive cholesterol was measured, as previously reported [30]. Phospholipid transfer protein activity using radiometric assay was carried out as described [33].

2.9 Quantitative real-time RT-PCR analyses

Liver RNA was isolated using the TRIzol® RNA isolation method (Gibco/BRL, Grand Island, NY, USA). Total RNA samples were repurified (RNeasy mini kit Plus; Qiagen, CA, USA) and checked for integrity by agarose gel electrophoresis. Total RNA (1 μg) was reverse-transcribed with Oligo(dT)$_{15}$ using M-MLV Reverse Transcriptase, RNase H Minus, Point Mutant (Promega Corporation, MD, USA) to generate cDNA. Predesigned validated primers (Assays-on-Demand; Applied Biosystems, Foster City, CA, USA) were used with TaqMan® probes. Real-time PCR assays were performed on a C1000 Thermal Cycler coupled to a CFX96 Real-Time System (Bio-Rad Laboratories SA, Life Science Group). All analyses were performed in duplicate and relative RNA levels were determined using glyceraldehyde 3-phosphate dehydrogenase (*Gapdh*) as an internal control.

2.10 Statistical methods

Data are expressed as medians (25th, 75th percentiles). Statistical analyses were performed using the Graphpad Prism software (GPAD, version 4.0, San Diego, CA, USA). Mann–Whitney *U* test was used to compare differences between groups. Comparisons of more than two groups were performed using Kruskal–Wallis nonparametric ANOVA test followed by Dunns multiple comparison test. The relationship between Hcy and HDL-C was tested using Spearman's correlation test. Differences between groups were considered statistically significant when $p < 0.05$.

3 Results

3.1 Effects of methionine-mediated HHcy on mouse and biochemical parameters

Mouse weight, food and water intake were similar in both the methionine-fed and the control female groups. No changes were observed in liver weight and plasma ALT enzyme activities did not differ between groups, whereas AST activity was slightly increased (1.1-fold) in plasma of hyperhomocysteinemic mice compared with control mice (Supporting Information Table 1). No differences were found either in total cholesterol dietary income or output between mouse groups (Supporting Information Table 2).

3.2 Effects of methionine-mediated HHcy on plasma and HDL

Feeding female mice with 1% methionine in water significantly (~7-fold) raised the fasting plasma Hcy concentrations [55.8 (38.3, 149.6) μM] of treated mice compared to control mice [8.2 (6.7, 9.3) μM] (Fig. 1). Methionine-induced HHcy was significantly lower [21.7 (11.0, 28.7) μM] in age-matched male mice than in female mice [55.8 (38.3, 149.6) μM] (Supporting Information Table 3). In contrast to male mice (Supporting Information Table 3), total plasma cholesterol was decreased in female hyperhomocysteinemic mice compared with female controls (Fig. 1). This was due to a significant drop in the plasma concentration of HDL-C (Fig. 1). HDL-C concentration was found to correlate significantly and negatively with plasma Hcy (Fig. 1).

Composition analysis of HDL isolated by sequential ultracentrifugation suggested that the drop in HDL-C was due to a decrease in plasma circulating HDL mass to approximately 16% with no change in the relative cholesterol content of HDL (Fig. 2A). Plasma Fast Protein Liquid Chromatography analysis confirmed that the HDL-C of female hyperhomocysteinemic mice was lower compared with control mice, with no changes in the cholesterol content of the other lipoprotein fractions (Fig. 2B). Kinetic analyses using radiolabeled [^{3}H]-cholesteryl oleate HDL indicated that methionine intake tended to raise ($p = 0.11$) the fractional catabolic rate of intravenously injected [^{3}H]-HDL (Fig. 2C). Further, the reduced HDL-C concentration in hyperhomocysteinemic female mice was mainly associated with an approximately 1.5-fold decrease in HDL synthesis rate (Fig. 2D). However, no significant changes in the recovery of HDL-derived [^{3}H]-cholesterol, expressed as percentage of the injected dose, in the livers [3.5 (3.3, 3.6)% in hyperhomocysteinemic mice versus 5.0 (4.2, 5.1)% in control mice; $p = 0.1143$] and feces [0.5 (0.4, 0.6)% in hyperhomocysteinemic mice versus 0.6 (0.5, 0.8)% in control mice; $p = 0.1143$] collected over a 24-h period were found between groups.

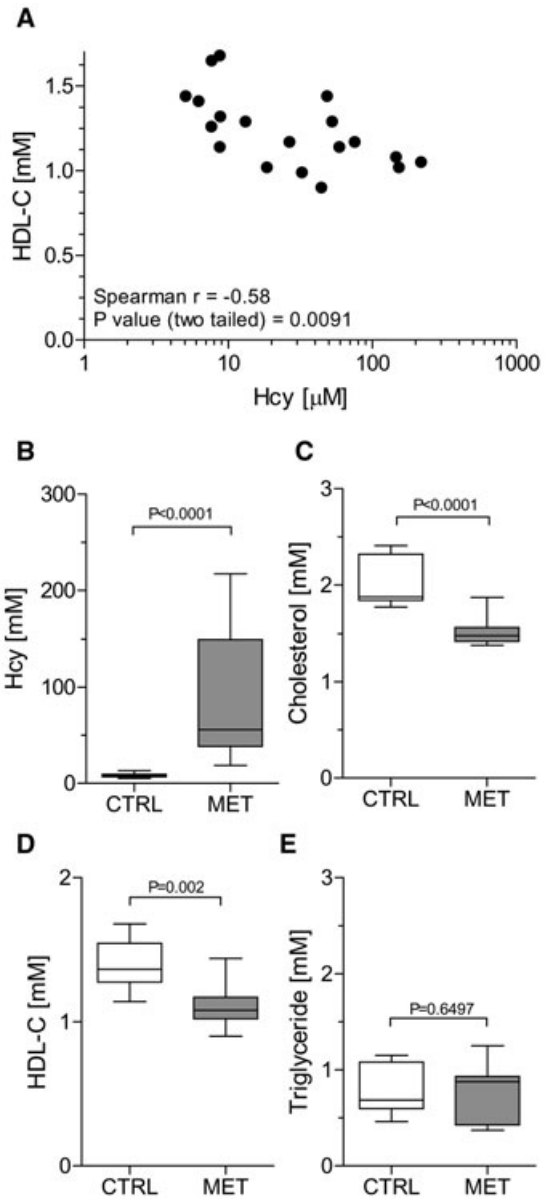

Figure 1. Effect of methionine-induced hyperhomocysteinemia (HHcy) on fasting plasma Hcy and lipid concentrations in fasting female C57BL/6NCrl mice. (A) Spearman correlation between fasting plasma Hcy and HDL-C concentrations. (B) Hcy plasma concentrations. (C) Plasma cholesterol concentrations. (D) HDL-C plasma concentrations. (E) Plasma triglyceride concentrations. All animal manipulations began at 2 p.m. with mice fasted for 6 h. Values are expressed as median (25th, 75th percentiles).

Serum samples from hyperhomocysteinemic female mice were incubated in the presence of an LCAT inhibitor to ascertain the potential of mouse serum to facilitate HDL particles interconversion. After 6 h of incubation, the percentage of pre-β-HDL in hyperhomocysteinemic mice [14.9 (12.1, 19.0)%] did not differ significantly from that shown by control mice [17.8 (14.7, 18.9)%]. A similar relative pre-β-HDL

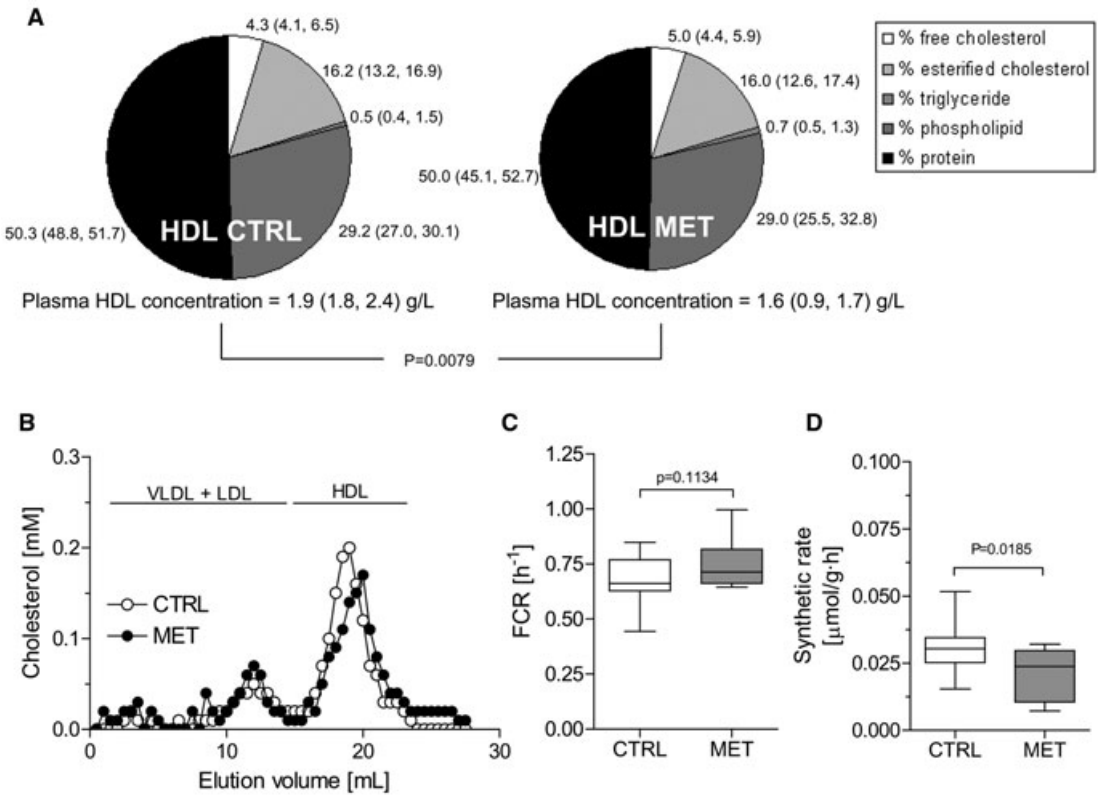

Figure 2. Effect of methionine-induced hyperhomocysteinemia (HHcy) on concentration and composition of circulating HDL and in vivo HDL turnover. (A) Schematic representation of composition and concentration of HDL isolated by ultracentrifugation from fasting plasma of hyperhomocysteinemic and control mice. Values represent median (25th, 75th percentiles) of five pools each composed of three to four mice. (B) Representative FPLC lipoprotein profiles obtained from pooled fasting plasma (five mice per group). (C) Fractional catabolic rate (FCR) of HDL-C (pools/h). Autologous HDL was isolated from pooled mouse plasma, labeled with [^{3}H]-cholesteryl oleate, and injected intravenously into mice. The radioactivity of HDL in blood 2-min postinjection is defined as 100%. FCR was calculated with data points for 6 h. (D) Synthetic rate of HDL-C (HDL-C μmol/g/h). HDL-C synthetic rate was calculated using the formula [(pool size × FCR)/g]. Values expressed as median (25th, 75th percentiles) ($n = 5$).

percentage distribution was found in male mice [hyperhomocysteinemic mice: 17.4 (15.0, 19.7)% versus control mice: 15.1 (13.2, 23.9)%].

3.3 Effects of hyperhomocysteinemic HDL on macrophage cholesterol efflux and in vivo macrophage-specific RCT

The ability of plasma and HDL from each mouse group to promote cholesterol efflux from [^{3}H]-cholesterol-labeled macrophages was evaluated. The efflux of cholesterol to total plasma and HDL of hyperhomocysteinemic mice was significantly lower than in controls (Fig. 3A and B). In an attempt to ascertain whether HHcy affected macrophage-dependent RCT in vivo, a minor fraction of the whole animal RCT, mice of each group were injected with radiolabeled macrophages. Plasma- and HDL-associated [^{3}H]-cholesterol in hyperhomocysteinemic female mice was also lower compared to control female mice after 48 h (Fig. 3C). The [^{3}H]-tracer recovery, expressed as percentage of injected dose, was also measured in liver and feces collected over a 48-h period. No significant changes were found between hyperhomocysteinemic and control mice (Fig. 3C). Macrophage-specific RCT, expressed as percentage of the injected dose in feces, remained unchanged in male mice [0.5 (0.5, 0.7)% in hyperhomocysteinemic mice versus 0.5 (0.4, 0.5)% in control mice; $p = 0.08$]. The effect of HHcy on intestinal cholesterol absorption in order to observe the transit of oral-gavaged, radiolabeled cholesterol into plasma, liver, gallbladder, small intestine, large intestine feces, and feces was also studied over a period of 48 h. The relative amount of [^{14}C]-cholesterol radioactivity in the above-mentioned compartments was found to be similar in both groups after 48 h (data not shown). Methionine-induced HHcy did not alter either the liver HDL-related gene expression of known RCT targets (i.e. *Sr-b1*, *Abca1*, *Abcg5*, *Abcg8*, *Cyp7a1*, *Lxrα*, and *Pparα*) compared to that of control mice (Supporting Information Fig. 1).

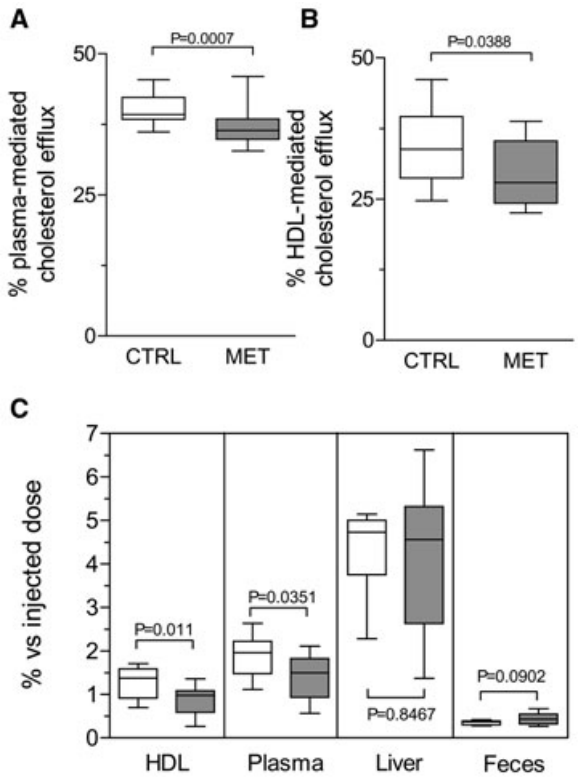

Figure 3. Effect of methionine-induced hyperhomocysteinemia HHcy on in vitro cholesterol efflux ability mediated by total plasma and plasma HDL and in vivo macrophage-specific reverse cholesterol transport (RCT). (A) Plasma-mediated and (B) HDL-mediated cholesterol efflux. Mouse plasma or HDL from apoB-depleted plasma were added to the culture medium of J774 cells loaded with [^{3}H]-cholesterol. The percentage of cholesterol efflux was determined. Values expressed as median (25th, 75th percentiles) (n = 8–10). (C) Individually housed mice were injected intraperitoneally with [^{3}H]-cholesterol-labeled J774 mouse macrophages ($\sim 3 \times 10^6$ cells containing approximately 1.0×10^6 cpm in 0.5 mL of saline in each mouse; cell viability was ~95%). The amount of [^{3}H]-tracer in plasma, HDL, liver, and feces is expressed as a fraction of the injected dose over 48 h. Values expressed as median (25th, 75th percentiles) (n = 8–10).

3.4 Effects of methionine-mediated HHcy on lipoprotein oxidation

The extent of copper-induced lipid oxidation was evaluated by measuring the conjugated diene formation in HDL isolated from female hyperhomocysteinemic and control groups (Fig. 4). HDL from hyperhomocysteinemic mice displayed a shorter lag phase, thereby indicating a lower resistance to oxidation (Fig. 4A). The ability of HDL to inhibit LDL oxidation was also tested by examining the conjugated diene formation of human LDL exposed to oxidative modification in the presence of HDL from each group (Fig. 4B). After the kinetics of HDL incubated without LDL were subtracted, HDL from hyperhomocysteinemic mice displayed a lesser ability to delay LDL oxidation compared with control mice. The relative electrophoretic mobility of LDL subjected to oxidation, which rises with oxidative modification, was increased in the presence of HDL from the hyperhomocysteinemic mice compared with that of control HDL (Fig. 4C). Known antioxidant HDL-associated proteins involved in HDL atheroprotective functions were also analyzed. First, plasma apoA-I concentration in hyperhomocysteinemic mice [0.7 (0.7, 0.8) g/L] was decreased compared with control mice [0.9 (0.8, 1.0) g/L; $p <$ 0.0001] (Fig. 4D) and this was not due to changes in apoA-I expression (Supporting Information Fig. 1). This observation was reconfirmed using mouse apoA-I-specific immunoblot analysis of native 4–20% polyacrylamide GGE to separate HDL (Fig. 4D, inset). This analysis showed that HDL from hyperhomocysteinemic mice presented fewer mouse apoA-I immunoreactive bands (lanes 4–6) compared with that of control mice (lanes 1–3). Second, plasma PON-1 activity was decreased in hyperhomocysteinemic mice [27.2 (26.1, 29.3) μmol/mL/min] compared with controls [30.4 (28.0, 31.9) μmol/mL/min, p = 0.0379] (Fig. 4E). Third, total plasma PAF-AH activity was decreased in hyperhomocysteinemic mice [93.3 (89.4, 99.6) nmol/mL/min] compared with controls [104.0 (97.9, 110.2) nmol/mL/min, p = 0.0377] (Fig. 4F). Changes in PON-1 and PAF-AH enzyme activities were even greater when determined in HDL obtained after precipitation of apoB-containing lipoproteins. In this case, PON-1 activity in HDL from hyperhomocysteinemic mice was 21.5 (16.9, 27.1) μmol/mL/min versus 31.6 (29.5, 33.6) μmol/mL/min in controls (p = 0.0159), whereas PAF-AH activity in HDL from hyperhomocysteinemic mice was 98.1 (83.6, 101.0) nmol/mL/min versus 111.4 (105.0, 121.2) nmol/mL/min in control mice (p = 0.0248). The differences in PON-1 and PAF-AH activities, which are thought to indicate changes in serum and HDL concentrations, were not explained either by changes in liver gene expression (Supporting Information Fig. 1). Finally, no significant changes in endogenous plasma LCAT activity [153.3 (125.8, 189.5) μmol/L/h in hyperhomocysteinemic mice versus 93.5 (70.4, 121.4) μmol/L/h in control mice; p = 0.1143] or plasma phospholipid transfer protein [14.9 (12.1, 19.0) μmol/mL/h in hyperhomocysteinemic mice versus 18.1 (14.8, 19.2) μmol/mL/h in control mice; p = 0.267] were found between groups. Most of the changes in the antioxidant HDL capacity of female mice were also found in male mice (Supporting Information Fig. 2).

4 Discussion

Meat, fish, and dairy products are good sources of methionine and their consumption have increased in Western societies [16]. Approximately half of dietary methionine is converted into Hcy [16]. Population and experimental studies demonstrated that high-protein or high-methionine feeding is associated with the development of HHcy and vascular disease [3, 9, 34]. Dysfunctional HDL particles with impaired atheroprotective functions have been reported to be present

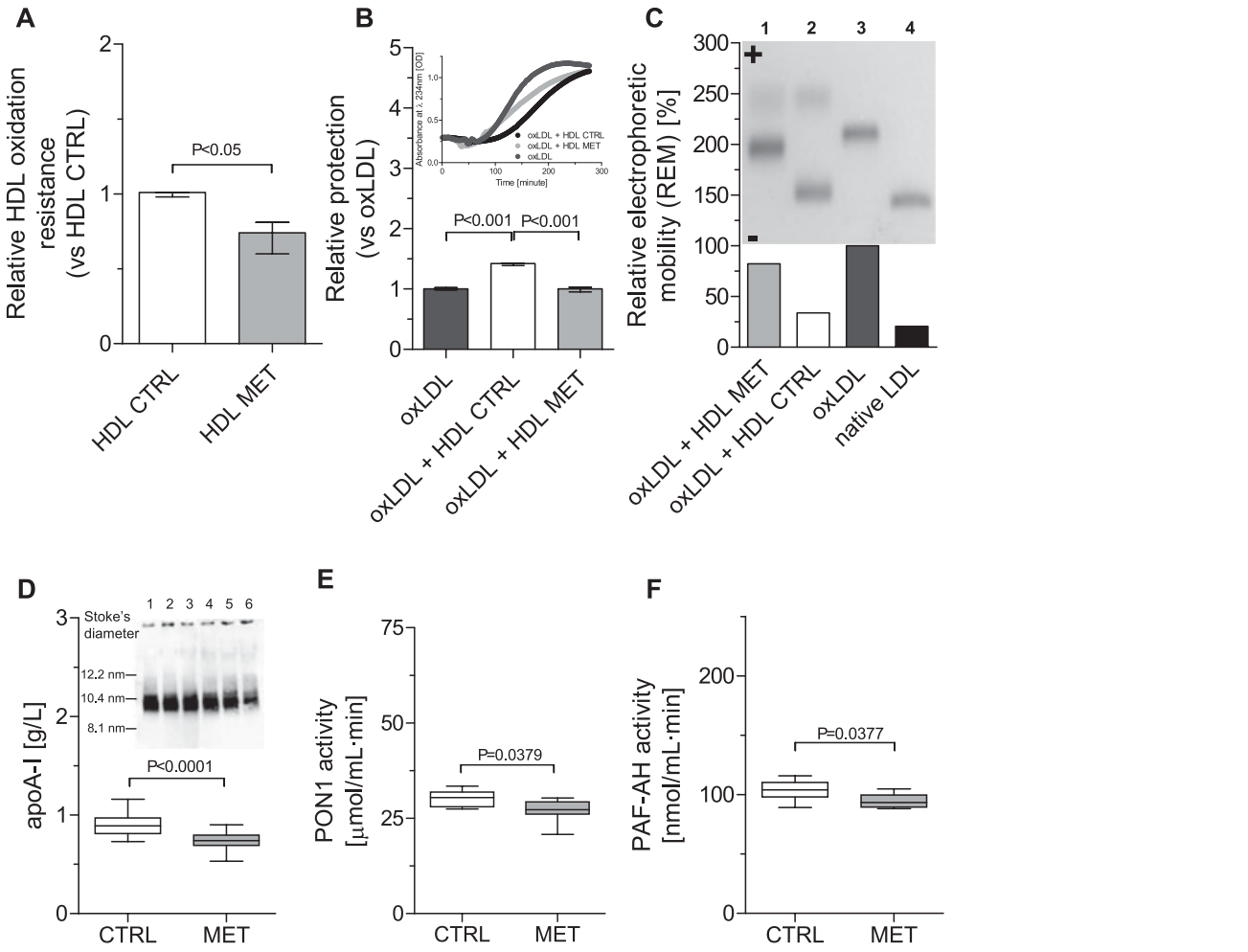

Figure 4. HDL oxidation resistance and related parameters in female mice. (A) Lag phase of conjugated diene formation in HDL co-incubated with 2.5 μM $CuSO_4$ at 37°C for 6 h. For calculations, the median lag time calculated for control HDL (19 min) was set at a normalized value of 1 arbitrary unit. (B) Lag phase of conjugated diene formation presented as relative lag phase to LDL kinetics oxidized without HDL. For calculations, the median lag time of oxLDL (71 min) was set at a normalized value of 1 arbitrary unit. Results are expressed as median (25th, 75th percentiles) of three independent pools of HDL obtained from five individual female mice per group. Inset, representative diene formation curves of LDL alone or with HDL coincubated with $CuSO_4$. (C) Analysis of human LDL relative electrophoretic mobility (REM) induced by exposure to $CuSO_4$ oxidation in the absence/presence of HDL. Inset, representative agarose gel electrophoretic mobilities of native and oxidized LDL in the absence (100% mobility) and presence of HDL are shown for comparison. (D) Plasma apoA-I concentration determined by ELISA. Inset, immunoblot analysis for mouse apoA-I of plasma HDL from control (lanes 1–3) and hyperhomocysteinemic mice (lanes 4–6) separated under native 4–20% gradient gel electrophoresis. (E) Plasma PON-1 activities. (F) Plasma PAF-AH activities. Values expressed as median (25th, 75th percentiles) ($n = 8$–10).

in plasma of hyperhomocysteinemic subjects in both humans and animal models [18, 20, 26]. However, in such studies, the atheroprotective function of hyperhomocysteinemic HDL analyzed was their in vitro ability to promote cholesterol efflux, the first step in RCT. On the other hand, HDL antioxidant capability was established by determining the expression or activity of known antioxidant HDL-associated enzymes in humans or mouse models [26]. Herein, we describe, for the first time to our knowledge, a thorough analysis of the in vivo effect of HHcy on macrophage-specific RCT and HDL protection against LDL oxidative modification.

Consistent with the previous data [9, 35], plasma concentration of Hcy was significantly elevated in the group supplemented with methionine in drinking water. HHcy achieved by increasing the total dietary methionine content up to approximately 13 g/kg did not result in significant changes in the body weight of our mice, with these results being in agreement with studies using similar animal models [2, 35, 36], but discordant with another study [25], which reported that methionine intakes >20 g/kg were associated with a significant weight loss (also reviewed in [9]). A possible explanation for such an effect could be the known untoward effects on growth

as well as other toxic effects previously described in mice fed with very-high-methionine diets [9]. In our study, total plasma cholesterol concentration was decreased in hyperhomocysteinemic mice mainly due to lower plasma HDL-C. These changes were not associated with alterations in HDL particle size or relative lipid or protein composition. Concurring with a previous report [25], increasing the dietary content of methionine was associated with a reduction in plasma HDL-C production, with a mild increase in HDL-C clearance contributing to the methionine-induced HDL deficiency [21]. Also, and consistent with previous observations, a decreased HDL production rate was associated with a reduced plasma concentration of apoA-I, an observation that could not be explained by changes in the liver at transcriptional level [20, 21]. In vitro pulse-chase experiments demonstrated that Hcy significantly reduced intracellular and secreted apoA-I protein, without altering mRNA, in mouse primary hepatocytes, thereby supporting the concept that Hcy inhibits apoA-I protein synthesis largely via translational regulation and this leads to an HDL reduction [20, 21].

HDL is central to RCT [19]. Within the RCT pathway, the ability of cholesterol efflux from cells to pre-β-HDL is known to be the first step in RCT, whereas LCAT-mediated esterification converts free cholesterol into its ester, leading to HDL maturation [19]. In our study, plasma activity and the liver expression of LCAT shown were not altered by HHcy, whereas total plasma and HDL from hyperhomocysteinemic mice displayed an impaired ability to promote cholesterol efflux from macrophages both in vitro and in vivo. This result concurs with one study performed in hyperhomocysteinemic humans [26] but not with a recent report using a subset of the FIELD study [37]. However, HHcy had no effect on the overall macrophage-to-feces cholesterol RCT pathway. It should be noted that RCT is a dynamic process and macrophage-derived cholesterol in intermediate compartments may not reflect the flux of cholesterol through different compartments. Consistent with these findings, no significant changes were observed either in the liver expression of genes mainly involved in RCT in hyperhomocysteinemic mice. Given the importance of the intestine in the net RCT flux [38], we also studied the effect of HHcy on intestinal cholesterol absorption. As previously described [25], the radiolabeled cholesterol content in different compartments of hyperhomocysteinemic mice was similar to that of control mice, indicating that methionine-induced HHcy did not impair cholesterol intestinal absorption.

The underlying mechanisms of HHcy toxicity caused by excessive methionine intake are poorly understood and have attracted a great deal of interest, with increased oxidative stress being considered as one of the potential contributors to atherosclerosis development [18]. Another crucial antiatherogenic function of HDL is its antioxidant protection of LDL. HDL are the main transporters of lipoperoxides in plasma, inhibit the formation of toxic lipid hydroperoxides and remove them from LDL, actions thought to be atheroprotective [39]. Oxidation is thought to impair HDL functions [39]; however, this may depend on the degree of oxidative modifications produced and/or on specific modifications produced by reactive species [40]. In our study, HDL isolated from plasma of hyperhomocysteinemic female, but not male, mice were prone to oxidation, possibly due to a sexual dimorphism as that described in relation to plasma lipoprotein metabolism and atherosclerosis susceptibility [41, 42]. However, hyperhomocysteinemic HDL from both female and male mice failed to protect LDL from oxidation compared with HDL of control mice. This was related to a reduction of HDL-associated antioxidant enzyme activities, PON-1 and PAF-AH, and plasma apoA-I in hyperhomocysteinemic female mice. Similar results were obtained in hyperhomocysteinemic male mice, with the exception of PAF-AH that did not differ significantly from that of control mice. This, therefore, would suggest that the decrease in PAF-AH is necessary, in addition to that of apoA-I and PON-1, to reduce HDL resistance to oxidation [43], but not to lose protection capacity against LDL oxidation. The sex differences found were probably related to the substantially higher plasma Hcy seen in females versus males when fed a methionine-enriched diet. It is noteworthy that one of the HDL proteins involved in antioxidant protection, PON-1, can cleave the highly reactive metabolite Hcy-thiolactone, which is increased in HHcy [44, 45]. PON-1 activity has been suggested to confer proteins protection against *N*-homocysteinylation which, in the case of HDL, might result in changes in the conformation and properties of its apos, including apoA-I, thus potentially affecting HDL protection against atherosclerosis [45]. Therefore, we suggest that a decrease in plasma PON-1 and PAF-AH activities and apoA-I concentration in the hyperhomocysteinemic mice impair the antioxidant properties of HDL. This HDL impairment during HHcy may, at least in part, be due to a decreased HDL mass secondary to reduced apoA-I synthesis. Although the translational mechanism(s) implicated in the reduction in apoA-I by HHcy remain unknown, recent data [46] show that enhanced endoplasmic reticulum stress, such as that triggered in HHcy [18], inhibits apoA-I secretion, possibly by affecting cellular degradation pathways but not apoA-I gene expression. Indeed, HDL has been shown to protect against endoplasmic reticulum stress [47].

Regarding the potential consequences of the HDL changes identified in the present study, it is worth noting that HDL also enhanced endothelium-dependent and nitric oxide dependent relaxation in mice arteries [48]. A reduction in the bioactivity of endothelial cell derived nitric oxide is a key step in the initiation and progression of atherosclerosis [49]. In the context of HHcy, an impaired antioxidant action of HDL could also be detrimental for endothelium relaxation through a decrease in nitric oxide availability [48]. Consistent with these data, the interaction of partial HDL deficiency and moderate HHcy in double heterozygous, apoA-I/CBS knockout mice concurred with a lower plasma nitric oxide concentration [34]. This suggests that the combination of both risk factors exacerbates endothelial dysfunction. In this context, impaired HDL protection against oxidation has also been observed in apoA-II transgenic mice, a mouse model of

insulin resistance and increased atherosclerosis susceptibility [50].

In conclusion, our data showed that methionine-induced HHcy did not affect the macrophage-specific RCT pathway in vivo, but did impair the protection of HDL against LDL oxidative modification in this animal model. These results indicate that HHcy might exert at least part of its pro-atherogenic effect by counteracting the antioxidant properties of HDL.

This work was funded by Ministerio de Sanidad y Consumo, Instituto de Salud Carlos III, FIS grants PI10/00277 (to J.J.), PI11/01076 (to F.B-V.), PI12/00291 (to J.C. E.-G.), Fundación Española de Arteriosclerosis grant—ALMIRALL 2010 (to F.B-V.), COST Action BM0904, and by the Research Council for Health, Academy of Finland (grant #257545 to M.J.). CIBER de Diabetes y Enfermedades Metabólicas Asociadas (CIBERDEM) is a project of the Instituto de Salud Carlos III. CIBER de Fisiopatología de la Obesidad y Nutrición is an initiative of the Instituto de Salud Carlos III. We are very grateful to Christine O'Hara for English revision of the manuscript. We also thank Antonia Rubio, Margarita Domingo, and Luis García Tato for animal healthcare and David Santos, Immaculada Porcel, Esther Cubero, Júlia Freixa, Jari Metso, and Sari Nuutinen for technical assistance.

The authors have declared no conflict of interest.

5 References

[1] Toborek, M., Hennig, B., Dietary methionine imbalance, endothelial cell dysfunction and atherosclerosis. *Nutr. Res.* 1996, *16*, 1251–1266.

[2] Zulli, A., Hare, D. L., High dietary methionine plus cholesterol stimulates early atherosclerosis and late fibrous cap development which is associated with a decrease in GRP78 positive plaque cells. *Int. J. Exp. Pathol.* 2009, *90*, 311–320.

[3] Metges, C. C., Barth, C. A., Metabolic consequences of a high dietary-protein intake in adulthood: assessment of the available evidence. *J. Nutr.* 2000, *130*, 886–889.

[4] Virtanen, J. K., Voutilainen, S., Rissanen, T. H., Happonen, P. et al., High dietary methionine intake increases the risk of acute coronary events in middle-aged men. *Nutr. Metab. Cardiovasc. Dis.* 2006, *16*, 113–120.

[5] Troen, A. M., Lutgens, E., Smith, D. E., Rosenberg, I. H. et al., The atherogenic effect of excess methionine intake. *Proc. Natl. Acad. Sci. USA* 2003, *100*, 15089–15094.

[6] Garlick, P. J., Toxicity of methionine in humans. *J. Nutr.* 2006, *136*, 1722S–1725S.

[7] Miller, R. A., Buehner, G., Chang, Y., Harper, J. M. et al., Methionine-deficient diet extends mouse lifespan, slows immune and lens aging, alters glucose, T4, IGF-I and insulin levels, and increases hepatocyte MIF levels and stress resistance. *Aging Cell* 2005, *4*, 119–125.

[8] Selhub, J., Homocysteine metabolism. *Annu. Rev. Nutr.* 1999, *19*, 217–246.

[9] Dayal, S., Lentz, S. R., Murine models of hyperhomocysteinemia and their vascular phenotypes. *Arterioscler. Thromb. Vasc. Biol.* 2008, *28*, 1596–1605.

[10] Finkelstein, J. D., Martin, J. J., Methionine metabolism in mammals. Adaptation to methionine excess. *J. Biol. Chem.* 1986, *261*, 1582–1587.

[11] Miller, J. W., Nadeau, M. R., Smith, J., Smith, D. et al., Folate-deficiency-induced homocysteinaemia in rats: disruption of S-adenosylmethionine's co-ordinate regulation of homocysteine metabolism. *Biochem. J.* 1994, *298*(Pt 2), 415–419.

[12] Malinow, M. R., Bostom, A. G., Krauss, R. M., Homocyst(e)ine, diet, and cardiovascular diseases: a statement for healthcare professionals from the Nutrition Committee, American Heart Association. *Circulation* 1999, *99*, 178–182.

[13] Selhub, J., Public health significance of elevated homocysteine. *Food Nutr. Bull.* 2008, *29*, S116–S125.

[14] Fay, W. P., Homocysteine and thrombosis: guilt by association? *Blood* 2012, *119*, 2977–2978.

[15] Williams, K. T., Schalinske, K. L., Homocysteine metabolism and its relation to health and disease. *Biofactors* 2010, *36*, 19–24.

[16] Steed, M. M., Tyagi, S. C., Mechanisms of cardiovascular remodeling in hyperhomocysteinemia. *Antioxid. Redox Signal.* 2011, *15*, 1927–1943.

[17] Zhou, J., Austin, R. C., Contributions of hyperhomocysteinemia to atherosclerosis: causal relationship and potential mechanisms. *Biofactors* 2009, *35*, 120–129.

[18] Perla-Kajan, J., Twardowski, T., Jakubowski, H., Mechanisms of homocysteine toxicity in humans. *Amino Acids* 2007, *32*, 561–572.

[19] Vergeer, M., Holleboom, A. G., Kastelein, J. J., Kuivenhoven, J. A., The HDL hypothesis: does high-density lipoprotein protect from atherosclerosis? *J. Lipid Res.* 2010, *51*, 2058–2073.

[20] Liao, D., Yang, X., Wang, H., Hyperhomocysteinemia and high-density lipoprotein metabolism in cardiovascular disease. *Clin. Chem. Lab. Med.* 2007, *45*, 1652–1659.

[21] Liao, D., Tan, H., Hui, R., Li, Z. et al., Hyperhomocysteinemia decreases circulating high-density lipoprotein by inhibiting apolipoprotein A-I protein synthesis and enhancing HDL cholesterol clearance. *Circ. Res.* 2006, *99*, 598–606.

[22] Mikael, L. G., Rozen, R., Homocysteine modulates the effect of simvastatin on expression of ApoA-I and NF-kappaB/iNOS. *Cardiovasc. Res.* 2008, *80*, 151–158.

[23] Taskinen, M. R., Sullivan, D. R., Ehnholm, C., Whiting, M. et al., Relationships of HDL cholesterol, ApoA-I, and ApoA-II with homocysteine and creatinine in patients with type 2 diabetes treated with fenofibrate. *Arterioscler. Thromb. Vasc. Biol.* 2009, *29*, 950–955.

[24] Mikael, L. G., Genest, J., Jr., Rozen, R., Elevated homocysteine reduces apolipoprotein A-I expression in hyperhomocysteinemic mice and in males with coronary artery disease. *Circ. Res.* 2006, *98*, 564–571.

[25] Velez-Carrasco, W., Merkel, M., Twiss, C. O., Smith, J. D., Dietary methionine effects on plasma homocysteine and HDL metabolism in mice. *J. Nutr. Biochem.* 2008, *19*, 362–370.

[26] Holven, K. B., Aukrust, P., Retterstol, K., Otterdal, K. et al., The antiatherogenic function of HDL is impaired in hyperhomocysteinemic subjects. *J. Nutr.* 2008, *138*, 2070–2075.

[27] National Research Council, *Guide for the Care and Use of Laboratory Animals*, The National Academies Press, Washington, DC 2011.

[28] Julve, J., Escola-Gil, J. C., Rotllan, N., Fievet, C. et al., Human apolipoprotein A-II determines plasma triglycerides by regulating lipoprotein lipase activity and high-density lipoprotein proteome. *Arterioscler. Thromb. Vasc. Biol.* 2010, *30*, 232–238.

[29] Escola-Gil, J. C., Llaverias, G., Julve, J., Jauhiainen, M. et al., The cholesterol content of Western diets plays a major role in the paradoxical increase in high-density lipoprotein cholesterol and upregulates the macrophage reverse cholesterol transport pathway. *Arterioscler. Thromb. Vasc. Biol.* 2011, *31*, 2493–2499.

[30] Marzal-Casacuberta, A., Blanco-Vaca, F., Ishida, B. Y., Julve-Gil, J. et al., Functional lecithin: cholesterol acyltransferase deficiency and high density lipoprotein deficiency in transgenic mice overexpressing human apolipoprotein A-II. *J. Biol. Chem.* 1996, *271*, 6720–6728.

[31] van Haperen, R., van Tol, A., Vermeulen, P., Jauhiainen, M. et al., Human plasma phospholipid transfer protein increases the antiatherogenic potential of high density lipoproteins in transgenic mice. *Arterioscler. Thromb. Vasc. Biol.* 2000, *20*, 1082–1088.

[32] Ribas, V., Sanchez-Quesada, J. L., Anton, R., Camacho, M. et al., Human apolipoprotein A-II enrichment displaces paraoxonase from HDL and impairs its antioxidant properties: a new mechanism linking HDL protein composition and antiatherogenic potential. *Circ. Res.* 2004, *95*, 789–797.

[33] Jauhiainen, M., Metso, J., Pahlman, R., Blomqvist, S. et al., Human plasma phospholipid transfer protein causes high density lipoprotein conversion. *J. Biol. Chem.* 1993, *268*, 4032–4036.

[34] Carnicer, R., Navarro, M. A., Arbones-Mainar, J. M., Arnal, C. et al., Genetically based hypertension generated through interaction of mild hypoalphalipoproteinemia and mild hyperhomocysteinemia. *J. Hypertens.* 2007, *25*, 1597–1607.

[35] Zhou, J., Werstuck, G. H., Lhotak, S., Shi, Y. Y. et al., Hyperhomocysteinemia induced by methionine supplementation does not independently cause atherosclerosis in C57BL/6J mice. *FASEB J.* 2008, *22*, 2569–2578.

[36] Yalcinkaya-Demirsoz, S., Depboylu, B., Dogru-Abbasoglu, S., Unlucerci, Y. et al., Effects of high methionine diet on oxidative stress in serum, apo-B containing lipoproteins, heart, and aorta in rabbits. *Ann. Clin. Lab. Sci.* 2009, *39*, 386–391.

[37] Maranghi, M., Hiukka, A., Badeau, R., Sundvall, J. et al., Macrophage cholesterol efflux to plasma and HDL in subjects with low and high homocysteine levels: a FIELD substudy. *Atherosclerosis* 2011, *219*, 259–265.

[38] Julve, J., Llaverias, G., Blanco-Vaca, F., Escola-Gil, J. C., Seeking novel targets for improving in vivo macrophage-specific reverse cholesterol transport: translating basic science into new therapies for the prevention and treatment of atherosclerosis. *Curr. Vasc. Pharmacol.* 2011, *9*, 220–237.

[39] Kontush, A., Chapman, M. J., Functionally defective high-density lipoprotein: a new therapeutic target at the crossroads of dyslipidemia, inflammation, and atherosclerosis. *Pharmacol. Rev.* 2006, *58*, 342–374.

[40] Gao, X., Jayaraman, S., Gursky, O., Mild oxidation promotes and advanced oxidation impairs remodeling of human high-density lipoprotein in vitro. *J. Mol. Biol.* 2008, *376*, 997–1007.

[41] Yang, X., Schadt, E. E., Wang, S., Wang, H. et al., Tissue-specific expression and regulation of sexually dimorphic genes in mice. *Genome Res.* 2006, *16*, 995–1004.

[42] Escola-Gil, J. C., Marzal-Casacuberta, A., Julve-Gil, J., Ishida, B. Y. et al., Human apolipoprotein A-II is a pro-atherogenic molecule when it is expressed in transgenic mice at a level similar to that in humans: evidence of a potentially relevant species-specific interaction with diet. *J. Lipid Res.* 1998, *39*, 457–462.

[43] Tellis, C. C., Tselepis, A. D., The role of lipoprotein-associated phospholipase A2 in atherosclerosis may depend on its lipoprotein carrier in plasma. *Biochim. Biophys. Acta* 2009, *1791*, 327–338.

[44] Perla-Kajan, J., Jakubowski, H., Paraoxonase 1 protects against protein N-homocysteinylation in humans. *FASEB J.* 2010, *24*, 931–936.

[45] Perla-Kajan, J., Jakubowski, H., Paraoxonase 1 and homocysteine metabolism. *Amino Acids* 2012, *43*, 1405–1417.

[46] Naem, E., Haas, M. J., Wong, N. C., Mooradian, A. D., Endoplasmic reticulum stress in HepG2 cells inhibits apolipoprotein A-I secretion. *Life Sci.* 2013, *92*, 72–80.

[47] Muller, C., Salvayre, R., Negre-Salvayre, A., Vindis, C., Oxidized LDLs trigger endoplasmic reticulum stress and autophagy: prevention by HDLs. *Autophagy* 2011, *7*, 541–543.

[48] Yuhanna, I. S., Zhu, Y., Cox, B. E., Hahner, L. D. et al., High-density lipoprotein binding to scavenger receptor-BI activates endothelial nitric oxide synthase. *Nat. Med.* 2001, *7*, 853–857.

[49] Kearney, M. T., Duncan, E. R., Kahn, M., Wheatcroft, S. B., Insulin resistance and endothelial cell dysfunction: studies in mammalian models. *Exp. Physiol.* 2008, *93*, 158–163.

[50] Castellani, L. W., Navab, M., Van Lenten, B. J., Hedrick, C. C. et al., Overexpression of apolipoprotein AII in transgenic mice converts high density lipoproteins to proinflammatory particles. *J. Clin. Invest.* 1997, *100*, 464–474.

